Photoluminescence study of solution-deposited Cu₂BaSnS₄ thin films

S. Levcenko, B. Teymur, D. B. Mitzi, et al.

open access

View Online   Export Citation   CrossMark

ARTICLES YOU MAY BE INTERESTED IN

Roadmap on organic–inorganic hybrid perovskite semiconductors and devices
APL Materials 9, 109202 (2021); https://doi.org/10.1063/5.0047616

Chinese Abstracts
Chinese Journal of Chemical Physics 34, i (2021); https://doi.org/10.1063/1674-0068/34/04/cabs

Momentum conservation in the Biot–Savart law
American Journal of Physics 89, 1033 (2021); https://doi.org/10.1119/10.0005207

APL Materials

SPECIAL TOPIC: Emerging Materials for Spin-Charge Interconversion

Read Now!

AIP Publishing

Photoluminescence study of solution-deposited Cu₂BaSnS₄ thin films

View Online   Export Citation   CrossMark

S. Levcenko,[1,2,a] B. Teymur,[3] D. B. Mitzi,[3,4] and T. Unold[1]

AFFILIATIONS

[1] Helmholtz-Zentrum für Materialien und Energie, Hahn-Meitner-Platz 1, 14109 Berlin, Germany
[2] Felix-Bloch-Institut für Festkörperphysik, Universität Leipzig, Linnéstraße 5, 04103 Leipzig, Germany
[3] Department of Mechanical Engineering and Materials Science, Duke University, Durham, North Carolina 27708, USA
[4] Department of Chemistry, Duke University, Durham, North Carolina 27708, USA

[a] Author to whom correspondence should be addressed: sergiu.levcenco@uni-leipzig.de

ABSTRACT

To experimentally identify the character of radiative transitions in trigonal Cu₂BaSnS₄, we conduct temperature and excitation intensity dependent photoluminescence (PL) measurements in the temperature range of 15–300 K. The low-temperature near band edge PL spectrum is interpreted as the free exciton at 2.11 eV and the bound exciton at 2.08 eV, coupled with associated phonon-assisted transitions. In the low energy region, we assign the dominant defect emission at 1.96 eV to donor–acceptor-pair recombination and the weak broad emission at 1.6 eV to the free-to-bound transition. The activation energies and temperature shift for the radiative transitions are determined and discussed. Above 90 K, the free exciton recombination becomes the dominant radiative transition, with its energy shift mainly governed by the contribution of optical phonons.

The earth-abundant Cu₂BaSnS₄ (CBTS) and Cu₂BaSnSe₄ (CBTSe) materials and their alloys Cu₂BaSn(S, Se)₄ (CBTSSe) have emerged as promising thin film absorbers for solar cell applications.[1–6] For devices based on sulfur–selenium alloys of these compounds with a bandgap of 1.55 eV, a photoconversion efficiency of 5.2% has been recently achieved.[1] The steep onset in the absorption spectra and the band edge luminescence at room temperature confirm the reduction of the band tailing and cation disorder in these Ba-based materials, which suggests possible superior optoelectronic properties compared to the kesterite compounds Cu₂ZnSn(S,Se)₄ (CZTSSe).[1–7] On the other hand, the defect states and the carrier recombination processes in the CBTSSe absorber, which play a crucial role in determining the actual device performance, are still poorly understood. Previous investigations have typically focused on the use of photoluminescence (PL) to quantify tail states in CBTSSe.[1–4] Most of these PL studies were carried out at room temperature, although some have been performed at low temperature.[2,3,8–10] Interestingly, at low temperature, the PL response of CBTS demonstrates the presence of excitonic effects, like what has been observed in stoichiometric chalcopyrite materials.[11,12] The character of the radiative transitions observed in the PL spectra of

CBTS at 79–300 K has been partially analyzed,[9] although questions regarding the spectrally overlapping excitonic luminescence remain unanswered. The aims of this paper are to report temperature-dependent PL over a wide temperature range of 15–300 K and to derive more detailed information regarding the exciton and defect related recombination properties of solution-processed films of the trigonal CBTS semiconductor.

CBTS thin films were deposited from dimethyl sulfoxide (DMSO)-based molecular inks with Ba-rich and Cu and Sn stoichiometric metal compositions via spin-coating of the inks onto Mo/soda lime glass substrates. The two different inks with (sample A) and without (sample B) NaCl added were prepared using a DMSO-based solvent. Our attempt at NaCl inclusion in the precursor solution for sample A stems from the hypothesis that sodium may positively influence the films' grain size, crystallization, and defect properties.[13–17] Detailed discussion regarding sample preparation, sample nomenclature, film purity (Fig. S1), and morphologic characterization (Fig. S2) is given in the supplementary material. Unless stated otherwise, here we discuss PL results on the final film referred as sample A. Although it has slightly improved morphology and larger grain size than sample B (Fig. S2), no significant

differences were noted in the photoluminescence properties between the samples with and without NaCl added to the solution. PL results on sample B are shown in the supplementary material (Figs. S3, S6–S8, and Table S1). Photoluminescence is excited using a 532-nm wavelength Nd:YAG laser and detected employing a 0.5 m grating monochromator coupled with a CCD camera. Wavelength calibration of the PL experimental system was performed with an Ar spectral calibration lamp. A set of neutral density filters was used to perform excitation intensity measurements in the range 0.06–25 W/cm^2. Temperature control was achieved in a closed-cycle cryogenic He cryostat operating in the range between 15 and 300 K. Note that sample temperature was measured with a silicon diode placed on top of an identical sample.

Figure 1(a) displays the low temperature PL spectrum of the CBTS sample measured at 15 K and an excitation intensity of 25 W/cm^2. A dominant narrow PL line at 2.08 eV with a full width at a half maximum (FWHM) of ~6 meV and a weaker PL line at 2.11 eV (FWHM of ~12 meV) can readily be identified in the near band edge region. Figure 1(b) shows the dependence of the intensity of these PL lines as a function of the excitation intensity (I_{exc}). As the excitation intensity increases, the intensity of the PL line at 2.08 eV increases super-linearly as $I_{exc}{}^m$ with $m = 1.1$, whereas the intensity of the PL line at 2.11 eV varies with the power coefficient of 1.0. At the same time, the energy positions of both PL lines are independent of I_{exc} (supplementary material, Fig. S4). Based on these findings and considering the theory for the excitation dependence of different types of PL transitions,[18] we attribute the PL line at 2.08 eV to a bound exciton (BE) transition, while we associate the PL line at 2.11 eV with the free exciton (FE) transition. Our interpretation is consistent with recent PL analysis,[9] which indicates the excitonic nature of the overlapped emissions in the near band edge PL at 79 K, although these transitions are located at apparently different energies in this prior work: a BE peak at ~2.038 eV and a FE transition at ~2.065 eV. However, other earlier PL reports showed excitonic emissions at ~2.07 and ~2.08 eV at 30 K,[2,3] in closer agreement with our result for the BE transition. In general, temperature may alter the energy of exciton transitions, but it has a negligible effect on the current transitions at least up to 80 K (shown below) and cannot account for the observed differences between our results and those reported in Ref. 9. We therefore believe that the differences are either due to different sample compositions/preparation routes or non-agreeing spectral calibrations of the measurement setups.

A closer inspection of the PL spectrum at 15 K reveals that the near band edge PL exhibits several additional weak transitions labeled by arrows in Fig. 1(a): at 2.046 and 2.055 eV on the high energy side of the 1.96 eV defect PL band and at 2.07 eV on the low energy side of the BE emission. In addition, two weak features at 2.10 and 2.125 eV accompany the FE emission. Each of these PL lines can be related to a different BE type transition or phonon replica[19] of the BE and FE emissions, except for the 2.125 eV transition. The latter emission can be associated with the excited state ($n = 2$) of the FE ($n = 1$, the ground exciton state) or a different free exciton (FE$_2$) transition originating from the lower energy state of the valence band. The assignment of phonon replica PL transitions is especially difficult due to the large number of the possible phonons in the vibrational spectrum of CBTS: 128 vibrational modes ranging from 72 cm^{-1} (~9 meV) to 413 cm^{-1} (~51 meV),[2] and still not all of them are known and identified. Nevertheless, a nearly equal energetic separation of ~10 meV between 2.046 and 2.055 eV PL lines, 2.07 eV PL line and BE, and 2.10 eV PL line and FE suggests that the low energy PL line in each pair can be associated with a LO (longitudinal optical) phonon replica of a higher energy PL line. Indeed, the known phonon modes[2] at 72 (~9 meV), 84 (~10 meV) and 93 cm^{-1} (~11 meV) have a close match to the found energetic difference of ~10 meV. Therefore, we assume that among the observed
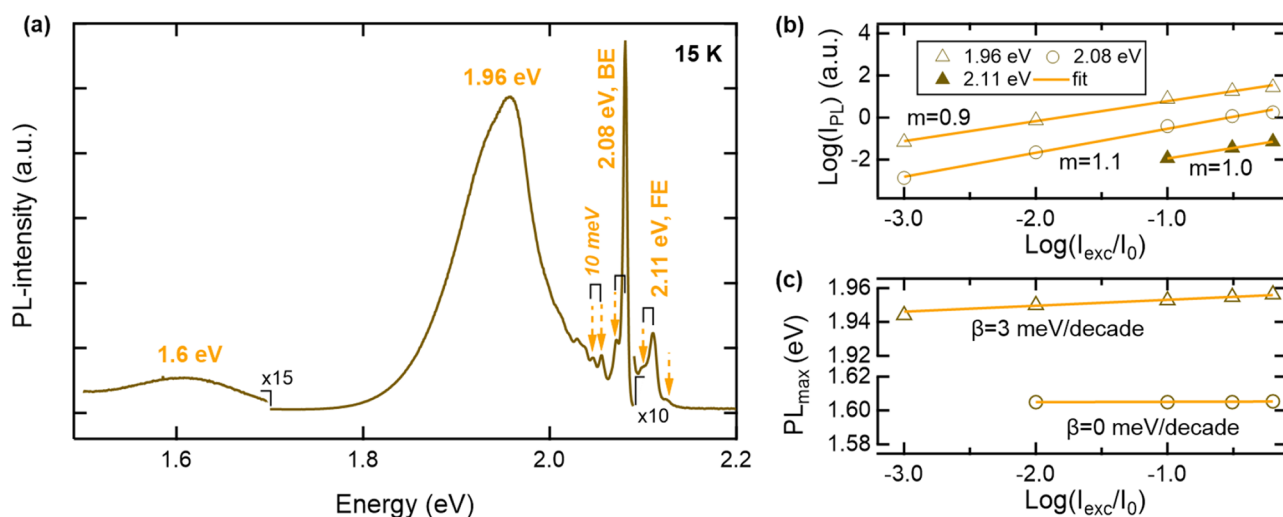
FIG. 1. (a) Photoluminescence (PL) spectrum of the CBTS film (sample A) measured at 15 K and excitation intensity of 25 W cm^{-2}. Arrows indicate several additional PL lines. Note that weak deep PL band at 1.6 eV was multiplied by factor of 15 and indicated as ×15. (b) The integrated PL intensity as a function of relative excitation power, I_{exc}/I_0, for different PL transitions, where $I_0 = 40$ W cm^{-2}. The solid lines represent the fits to $I_{PL} \sim (I_{exc}/I_0)^m$, where m is the power coefficient. (c) PL maximum as a function of I_{exc}/I_0 for defect PL transitions. The solid lines are the fits to $PL_{max} \sim \beta \log(I_{exc}/I_0)$, where β is the rate constant.

TABLE I. Peak energies of the near band edge PL for the CBTS film.

Peak (eV)	Assignment	Peak (eV)	Assignment	Peak (eV)	Assignment
	This work (15 K)		References 2 and 3 (30 K)		Reference 9 (79 K)
2.125	FE (n = 2) or FE$_2$				
2.11	FE			2.065	FE
2.10	FE-LO				
2.08	BE	2.07, 2.08	Exciton	2.038	BE
2.07	BE-LO				
2.055	BE$_2$				
2.046	BE$_2$-LO				

weaker PL lines, only the 2.055 eV line may relate to a second bound exciton (BE$_2$) transition, while the other lines likely correspond to phonon replicas. Table I summarizes the peak energies of the near band edge PL emissions and our plausible assignments, along with comparisons to available literature data.

We now turn to defect related emissions, presented by the relatively intense asymmetric (FWHM of ~0.11 eV) PL band at 1.96 eV and the weak broad (FWHM of ~0.15 eV) PL band at 1.6 eV in the low temperature PL spectrum [Fig. 1(a)]. The intensity variation of these PL bands with I_{exc} is sublinear: $m = 0.9$ for the 1.96 eV PL band [Fig. 1(b)] and $m = 0.8$ for the 1.6 eV PL band (supplementary material, Fig. S5). The PL band at 1.96 eV shifts to higher energy with increasing I_{exc}, showing a rate constant β of 3 meV/decade, but the maximum of the PL band at 1.6 eV stays constant [see Fig. 1(c)]. Based on these observations, we interpret the PL band at 1.96 eV as arising from donor–acceptor pair (DAP) transitions.[20] The weak broad lower energy PL band is assigned to a free-to-bound (FB) transition,[21] where a deep acceptor or donor with the defect level energy of about 0.5 eV is involved. Note that a similar defect PL band peaked

in the range of 1.95–1.99 eV was observed and interpreted as arising from either free-to-bound or DAP transitions[2,3] or even from a mixed character.[9] Comparing the small value of $\beta = 3$ meV/decade for the defect PL band (at 1.96 eV) in CBTS with the large value of $\beta = 12$ meV/decade for the defect PL band at 1.5 eV in CBTSSe,[10] we conclude that potential fluctuations play a relatively less important role in CBTS.

To further elucidate the mechanism of radiative recombination, we examined the temperature evolution of the PL spectrum. In Fig. 2(a), we illustrate the normalized PL spectra for several temperatures in the range from 15 to 300 K. The principal features of the PL spectra are the complete thermal quenching of the dominant PL transitions (BE at 2.08 eV and DAP at 1.96 eV) with increasing temperature. For temperatures above 55 K, the PL intensity of the BE transition is lower than the intensity of the FE transition, which becomes the dominant transition above 90 K. At temperatures above 75 K, the signal of the BE transition is strongly quenched and does not allow us to further follow its temperature dependence. In Fig. 2(b), the integrated intensity of BE and FE transitions vs
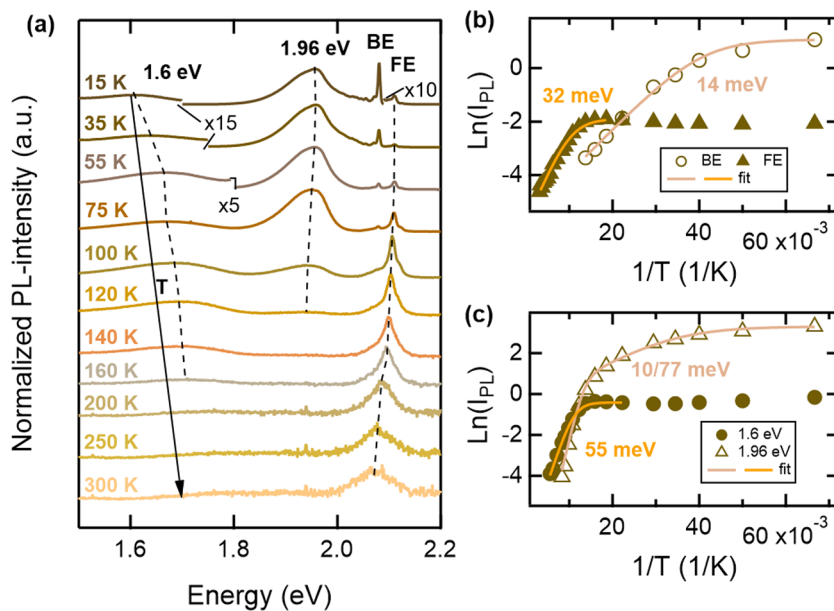
FIG. 2. (a) Normalized photoluminescence (PL) spectra of the CBTS film (sample A) measured at different temperatures and an excitation intensity of 25 W cm^{-2}. Note that some weak PL bands were multiplied by factors of 5, 10, and 15 and indicated as ×5, ×10, and ×15, respectively. The temperature quenching of the (b) BE and FE bands and (c) defect related PL bands.

reciprocal temperature are plotted and analyzed with a model assuming one nonradiative recombination pathway,[22]

$$I(T) = \frac{I_0}{1 + \alpha \exp\left(-\frac{E_{act}}{k_B T}\right)}, \quad (1)$$

where I_0 is the intensity extrapolated to T = 0 K, α is the process rate parameter, k_B is the Boltzmann constant, and E_{act} is the activation energy. A fit to the data yields activation energies of ~14 and 32 meV for BE and FE transitions, respectively.

For a direct bandgap semiconductor with simple parabolic isotropic valence and conduction bands, the energies of the FE transitions are given by $E_{ex}^n = E_g - E_b/n^2$, where E_g is the bandgap, E_b is the exciton binding energy, and n is the principal quantum number.[23] The exciton binding energy can be calculated as $E_b = \mu e^4/2\hbar^2\varepsilon^2$, where $\mu = m_h m_e/(m_h + m_e)$ is the reduced mass, m_h (m_e) is the effective hole (electron) mass, $\hbar$ is the reduced Planck constant, and ε is the static dielectric constant. A difficulty in calculating the exciton parameters of CBTS is that the required material parameters are experimentally unknown, and only theoretical values of these parameters can be found in the literature.[1,2,5,9] We estimate that the value of E_b lies in the range of 50–60 meV, based on the geometric means of the theoretical hole and electron effective masses,[24] $0.19 < m_e^* < 0.21$, and $0.57 < m_h^* < 0.64$, respectively, in units of free electron mass,[1,5] and the theoretical value of $\varepsilon = 6.1$.[9] However, comparing the result for CBTS and the exciton binding energy of common III-V and I-III-VI$_2$ chalcopyrite materials,[23] we find that the deduced E_b value of the former compound is at least 20–30 meV higher than the values observed in semiconductors with similar E_g of ~2.0 eV, and thus, it should be considered as a rough estimation. In contrast, the obtained experimental value E_{act} = 32 meV of the FE emission is assigned to be the exciton binding energy, which is in good agreement with experimental values in semiconductors with similar bandgap.[23]

Although there are several formation mechanisms for bound excitons in semiconductors, the mass ratio $\sigma = m_e^*/m_h^* \approx 0.33$ of CBTS implies that neither an ionized acceptor nor an ionized donor can be involved in the formation of the bound exciton.[24] In contrast, a neutral (non-ionized) defect (acceptor or donor) might be responsible for the observation of BE emission at 2.08 eV.[25] From the energy difference between the FE and BE transition energies, $\Delta E = E_{FE} - E_{BE} \approx 0.03$ eV, we evaluate the energy level of the involved neutral defect. Considering $\sigma \approx 0.33$, theory provides[25] the following expressions: $\Delta E = 0.11 E_A$ and $\Delta E = 0.21 E_D$, where E_A and E_D are the acceptor and donor level energies, respectively. Thus, BE emission at 2.08 eV can be either related to an acceptor level of 0.27 eV or to a donor level of 0.14 eV in CBTS. It is interesting to note that these obtained E_A and E_D energies are comparable with simple estimates from the hydrogenic approximation ($E_D = 13.6/\varepsilon^2 m_e^*$ eV and $E_A = 13.6/\varepsilon^2 m_h^*$ eV),[26] yielding 0.21–0.23 eV for an acceptor and 0.07–0.08 eV for a donor. Recent density functional theory (DFT) calculations with the HSE06 functional have shown the shallowest transitions E_A ~ 0.06 eV originating from V$_{Cu}$ (Cu vacancy) and E_D ~ 0.12 eV caused by Cu$_i$ (Cu interstitial).[9] The obtained value of E_{act} ≈ 14 meV for the BE recombination is lower than $\Delta E \approx 0.03$ eV and could be attributed to the dissociation of the bound exciton into the free hole (electron) and bound exciton at charged acceptor (donor) defects or to the formation of free excitons.[27] However, the former

dissociation process is less likely as charged defects do not attract free excitons in a semiconductor with $\sigma = m_e^*/m_h^* \approx 0.33$,[24] while the later process is supported by the enhancement of the FE emission over 15–50 K [Fig. 2(b)].

Figure 2(c) depicts an Arrhenius plot analysis of defect related transitions. Clearly, two activation energies are needed to fit the thermal quenching of the DAP transition at 1.96 eV: the low temperature region (15 K < T < 60 K) is characterized with $E_{act1} \approx 10$ meV and the high temperature region (60 K < T < 110 K) is described with $E_{act2} \approx 77$ meV. In the low temperature region, the energy of the DAP transition is nearly constant at fixed excitation power [Fig. 2(a)] and no new PL band at high energy emerges during the quenching process. From this observation, we conclude that E_{act1} corresponds to the activation of a competitive nonradiative path and does not represent the energy of the defect involved in DAP recombination. In contrast, E_{act2} can be attributed to the acceptor or donor defect of DAP recombination. When the defect involved in the DAP transition is ionized, the transformation from the DAP to FB type occurs.[11,28] A lack of observation of this transformation in our experiment can be explained by a small recombination probability of the FB transition between the electron bound to a donor level and a free hole in a valence band for a p-type semiconductor.[29] Thus, we propose that E_{act2} corresponds to thermal ionization of acceptor, E_A, consistent with the theoretical result for V$_{Cu}$.[9] Within the uncertainty of the Coulomb term, E_Q, involved in the energy of DAP transition,[20] $E_{DAP} = E_g - E_A - E_D + E_Q$, we can estimate the energy of the donor level, E_D, by using our experimentally inferred exciton binding energy ($E_b \approx 0.03$ eV) as $E_D = E_{FE} + E_b - E_{DAP} - E_{act2} \approx 0.1$ eV. The obtained result is in good agreement with the theoretical value of the donor originating from the Cu$_i$ lattice defect.[9] It is interesting to note that the extracted value for the donor level is comparable to the above given estimate (0.14 eV) of the donor level involved in the formation of the BE emission at 2.08 eV and thus allows us to assign the BE emission to a neutral donor bound exciton. A plausible scheme of the shallow defect and exciton PL transitions is summarized in Fig. 3. The determined defect energies from the studied CBTS thin films (samples A and B) and literature values are listed in Table II.

The deep FB transition at 1.6 eV strongly quenches in the range of 70–160 K with $E_{act} \approx 55$ meV. This small activation energy cannot correspond to a deep defect involved in the FB transition, and
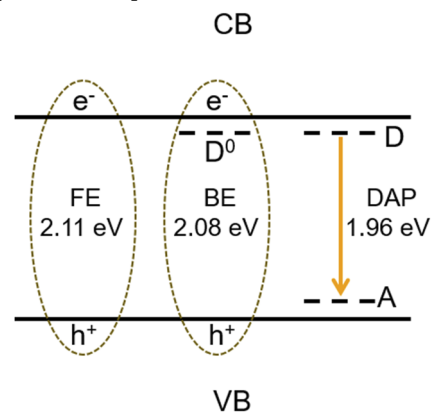
FIG. 3. A schematic drawing of the shallow defect and exciton transitions in CBTS.

TABLE II. Defect energies for the CBTS film.

Type	Experiment Energy (meV)		Theory[a] Energy (meV)	Origin
Acceptor	77–94[b]	39–45[a]	63	V_{Cu}
Donor	92–105[b]	129–144[a]	118	Cu_i
Deep defect	500[b]	300[a]	⋯	⋯
Deep defect	⋯	700[a]	⋯	⋯

[a]Reference 9.
[b]Present work.

we relate it to the activation of a competitive nonradiative channel. The simple model for FB recombination,[21,28] which describes the effect of T on the transition energy as $E_{FB} = E_g − E_A + k_B T/2$, cannot adequately explain the observed strong blue shift for the PL maximum with increasing T: a blue shift by about 60 meV in the range of 15–50 K and a gradual increase by 40 meV up to 160 K (see Fig. 4). The precise mechanism by which recombination occurs remains unclear, but it resembles the temperature characteristics of the deep PL transitions near grain boundaries and dislocations observed in CuGaTe$_2$.[30] Further sub-micrometer resolved PL or cathodoluminescence measurements would be useful to further clarify the properties and the origin of this deep PL band but were not within the scope of this study. Note that our results for defect related PL differ in activation energies and in the temperature regions of thermal quenching from the recent analysis,[9] presumably due to the differences in sample composition and preparation conditions or to the higher excitation power used in their PL experiment.

Finally, we analyzed the temperature dependence of the FE energy based on a model with a Bose–Einstein type occupation

FIG. 4. Photoluminescence (PL) maxima as a function of temperature for different PL transitions of the CBTS film (sample A) measured at an excitation intensity of 25 W cm^{-2}. The solid line is the fit based on the Bose–Einstein model, and the dashed line is the fit from Ref. 2.

function given by[31]

$$E_{FE}(T) = E_0 − A\left[\frac{2}{\exp\left(\frac{\theta}{T}\right) − 1} + 1\right], \quad (2)$$

where E_0 is the fit energy, θ is the temperature corresponding to the average phonon temperature, and A is the weight constant. The theoretical curve agrees well with the experimental data (see Fig. 4), and the nonlinear square fit yields θ = 280 K, E_0 = 2.144 eV, and A = 0.034 eV. The calculated value of θ is consistent with the average phonon temperature of ~314 K obtained by calculating the arithmetic mean of the 20 Raman active modes of CBTS,[2] indicating that the optical phonons contribute mainly to the shift of the FE energy with temperature. For the temperatures above θ, the linear slope of the FE energy can be evaluated[32] as $\frac{dE_{FE}}{dT} = −\frac{2A}{\theta}$ ≈ −0.24 eV/K. Under the assumption that the exciton binding energy (E_b) is temperature-independent, which is normally the case for chalcopyrite compounds,[33] the value for the linear shift in E_{FE} at high temperatures is also valid for the temperature dependence of the bandgap energy. Our value of the linear shift in E_{FE} is lower than the reported value of −0.37 eV/K, which is determined from analysis of ellipsometry data measured in the high temperature range of 280–500 K for sputtered CBTS films.[2] In Fig. 4, the empirical linear relationship $E_g(T) = 2.068 − 3.7 × 10^{−4} × (T − 296)$ from Ref. 2 is also plotted. A comparison shows a pronounced discrepancy from the experimental FE data, indicating that this equation must be applied with caution, especially at low temperatures. Note that this linear equation is also in clear contradiction with other analytical descriptions that predict significantly weaker dependency on temperature for the bandgap and excitonic energies in the low temperature region.[33,34]

It is interesting to briefly compare luminescence properties of previously studied and related CBTSSe films[10] with the current study on CBTS films. Despite a similar stoichiometry for CBTSSe and CBTS samples, we observe a distinct difference in PL behavior. For CBTSSe samples, the excitonic luminescence is absent and only the defect related PL dominates at low temperature. A similar difference in PL behavior is commonly seen for chalcopyrite Cu(In, Ga)Se$_2$ semiconductors, where stoichiometric samples of high electronic quality exhibit a narrow excitonic luminescence signal along with shallow and deep defect PL signatures, while the broad defect related PL is found in Cu-poor samples with a high density of structural defects and consequently potential fluctuation effects.[11,12] Note that potential fluctuation effects are also observed in kesterite CZTSSe, and it is usually attributed to the inhomogeneous distribution of charged defects and compositional fluctuations.[35] It is unclear if the PL differences between CBTSSe and CBTS are due to compositional effects or to possible variations of the defect properties or electronic band structure. However, an improved understanding of the discussed PL differences in the CBTSSe family is expected from future studies.

In summary, the radiative recombination processes in solution-processed CBTS films have been investigated using steady state PL spectroscopy in the temperature range of 15–300 K. The near band edge PL consists of spectrally distinct emission lines at 2.08 and at 2.11 eV, related to the bound exciton and the free exciton, respectively, as well as of additional weak PL lines that are particularly observed at low temperature. Most of these additional PL lines are
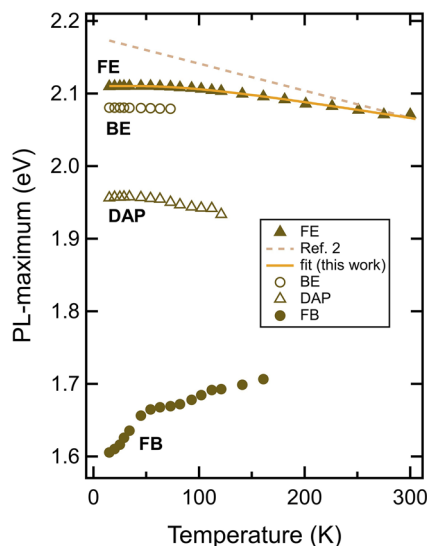
linked to phonon replicas of the exciton transitions. The defect luminescence exhibits the strongest broad emission at 1.96 eV, related to donor–acceptor-pair recombination, and a weak broad band at 1.6 eV, the origin of which is assigned to a deep defect presumably located at the grain boundaries and/or dislocations. We further considered thermal quenching of the defect and excitonic transitions and determined their activation energies. An analytical model based on Bose–Einstein statistics describes well the variation of free exciton energy with temperature and reveals that optical phonons contribute to its temperature shift.

See the supplementary material for sample preparation details, XRD and SEM data, additional PL data on sample A, and PL data on sample B.

AUTHOR DECLARATIONS
Conflict of Interest

The authors have no conflicts of interest to disclose.

DATA AVAILABILITY

The data that support the findings of this study are available from the corresponding author upon reasonable request.

REFERENCES

[1] D. Shin, T. Zhu, X. Huang, O. Gunawan, V. Blum, and D. B. Mitzi, Adv. Mater. **29**, 1606945 (2017).

[2] J. Ge, P. Koirala, C. R. Grice, P. J. Roland, Y. Yu, X. Tan, R. J. Ellingson, R. W. Collins, and Y. Yan, Adv. Energy Mater. **7**, 1601803 (2017).

[3] J. Ge, P. J. Roland, P. Koirala, W. Meng, J. L. Young, R. Petersen, T. G. Deutsch, G. Teeter, R. J. Ellingson, R. W. Collins, and Y. Yan, Chem. Mater. **29**, 916 (2017).

[4] B. Teymur, Y. Zhou, E. Ngaboyamahina, J. T. Glass, and D. B. Mitzi, Chem. Mater. **30**, 6116 (2018).

[5] M. Pandey and K. W. Jacobsen, Phys. Rev. Mater. **2**, 105402 (2018).

[6] D. Shin, B. Saparov, T. Zhu, W. P. Huhn, V. Blum, and D. B. Mitzi, Chem. Mater. **28**, 4771 (2016).

[7] F. Hong, W. Lin, W. Meng, and Y. Yan, Phys. Chem. Chem. Phys. **18**, 4828 (2016).

[8] A. Crovetto, Z. Xing, M. Fischer, R. Nielsen, C. N. Savory, T. Rindzevicius, N. Stenger, D. O. Scanlon, I. Chorkendorff, and P. C. K. Vesborg, ACS Appl. Mater. Interfaces **12**, 50446 (2020).

[9] A. Crovetto, S. Kim, M. Fischer, N. Stenger, A. Walsh, I. Chorkendorff, and P. C. K. Vesborg, Energy Environ. Sci. **13**, 3489 (2020).

[10] B. Teymur, S. Levcenco, H. Hempel, E. Bergmann, J. A. Márquez, L. Choubrac, I. G. Hill, T. Unold, and D. B. Mitzi, Nano Energy **80**, 105556 (2021).

[11] A. Bauknecht, S. Siebentritt, J. Albert, and M. C. Lux-Steiner, J. Appl. Phys. **89**, 4391 (2001).

[12] S. Zott, K. Leo, M. Ruckh, and H.-W. Schock, J. Appl. Phys. **82**, 356 (1997).

[13] M. Werner, C. M. Sutter-Fella, Y. E. Romanyuk, and A. N. Tiwari, Thin Solid Films **582**, 308 (2015).

[14] M. Werner, C. M. Sutter-Fella, H. Hagendorfer, Y. E. Romanyuk, and A. N. Tiwari, Phys. Status Solidi A **212**, 116 (2015).

[15] C. M. Sutter-Fella, J. A. Stückelberger, H. Hagendorfer, F. La Mattina, L. Kranz, S. Nishiwaki, A. R. Uhl, Y. E. Romanyuk, and A. N. Tiwari, Chem. Mater. **26**, 1420 (2014).

[16] Q. Guo, G. M. Ford, R. Agrawal, and H. W. Hillhouse, Prog. Photovoltaics **21**, 64 (2013).

[17] T. Gershon, B. Shin, N. Bojarczuk, M. Hopstaken, D. B. Mitzi, and S. Guha, Adv. Energy Mater. **5**, 1400849 (2015).

[18] T. Schmidt, K. Lischka, and W. Zulehner, Phys. Rev. B **45**, 8989 (1992).

[19] K. Yoshino, T. Ikari, S. Shirakata, H. Miyake, and K. Hiramatsu, Appl. Phys. Lett. **78**, 742 (2001).

[20] P. J. Dean and J. L. Merz, Phys. Rev. **178**, 1310 (1969).

[21] D. M. Eagles, J. Phys. Chem. Solids **16**, 76 (1960).

[22] M. Leroux, N. Grandjean, B. Beaumont, G. Nataf, F. Semond, J. Massies, and P. Gibart, J. Appl. Phys. **86**, 3721 (1999).

[23] B. Gil, D. Felbacq, and S. F. Chichibu, Phys. Rev. B **85**, 075205 (2012).

[24] R. R. Sharma and S. Rodriguez, Phys. Rev. **153**, 823 (1967).

[25] H. Atzmüller, F. Fröschl, and U. Schröder, Phys. Rev. B **19**, 3118 (1979).

[26] E. Zacks and A. Halperin, Phys. Rev. B **6**, 3072 (1972).

[27] D. Bimberg, M. Sondergeld, and E. Grobe, Phys. Rev. B **4**, 3451 (1971).

[28] A. Yamada, P. Fons, S. Niki, H. Shibata, A. Obara, Y. Makita, and H. Oyanagi, J. Appl. Phys. **81**, 2794 (1997).

[29] J. Krustok, J. H. Schön, H. Collan, M. Yakushev, J. Mädasson, and E. Bucher, J. Appl. Phys. **86**, 364 (1999).

[30] J. Krustok, J. Raudoja, M. Yakushev, R. D. Pilkington, and H. Collan, J. Appl. Phys. **86**, 5305 (1999).

[31] S. Logothetidis, M. Cardona, P. Lautenschlager, and M. Garriga, Phys. Rev. B **34**, 2458 (1986).

[32] A. Meeder, A. Jäger-Waldau, V. Tezlevan, E. Arushanov, T. Schedel-Niedrig, and M. C. Lux-Steiner, J. Phys.: Condens. Matter **15**, 6219 (2003).

[33] J. Bhosale, A. K. Ramdas, A. Burger, A. Muñoz, A. H. Romero, M. Cardona, R. Lauck, and R. K. Kremer, Phys. Rev. B **86**, 195208 (2012).

[34] R. Pässler, Phys. Status Solidi B **200**, 155 (1997).

[35] M. Grossberg, J. Krustok, C. J. Hages, D. M. Bishop, O. Gunawan, R. Scheer, S. M. Lyam, H. Hempel, S. Levcenco, and T. Unold, J. Phys. Energy **1**, 044002 (2019).